Dynamic modelling of an Organic Rankine Cycle applied to electricity production by the mean of Ocean Thermal Energy Conversion (OTEC)

Alexandre Dijoux, Frantz Sinama, Olivier Marc Marc, Bertrand Clauzade, Jean Castaing-Lasvignottes

Dynamic modelling of an Organic Rankine Cycle applied to electricity production by the mean of Ocean Thermal Energy Conversion (OTEC)

Authors

Alexandre Dijoux[a b*], Frantz Sinama[a], Olivier Marc[a], Bertrand Clauzade[b] and Jean Castaing-Lasvignottes[a]

[a]Laboratory of Physical and Mathematical Engineering for Energy, Environment and Building (PIMENT), University of Reunion Island,
40 Avenue de Soweto, 97400 Saint-Pierre, Reunion Island, France
[b]NAVAL ENERGIES,
Indret, 44620 La Montagne, France
**Corresponding Author: alexandre.dijoux@univ-reunion.fr*

ABSTRACT

Ocean Thermal Energy Conversion (OTEC) consists in using the temperature difference between hot surface seawater and cold deep seawater as an energy resource. This latter is often considered to be used as a stable base mean for electricity production. This study presents a dynamic model of an Organic Rankine Cycle (ORC) applied to OTEC, by using a Moving Boundary Model (MBM) for heat exchangers. This model consists in dividing the evaporator into three variant size parts (heating, evaporation and overheating) as well as the condenser (desuperheating, condensation and subcooling). Temperature variations in both working fluid and seawater side were computed. The response of the system following a step change in working fluid mass flow rate is then studied by considering input parameters from an OTEC onshore prototype located in Reunion Island. The output power of the system is then decreasing from 15.7 kW to 13.7 kW in a time lower than two minutes, after a decrease in working fluid mass flow rate by 25 %. This results show that the power of an OTEC power plant can be modulated with relatively short response times and it is therefore possible to consider using OTEC not only as a base resource, but also as a way to regulate the network in critical periods, particularly for non-connected grids.

Keywords: Ocean Thermal Energy Conversion (OTEC), Organic Rankine Cycle (ORC), Dynamic Modelling, Moving Boundary Model.

1 INTRODUCTION

Ocean Thermal Energy Conversion (OTEC) is known as a renewable, environment-friendly, and particularly steady and non-intermittent energy resource [1], [2]. It consists in using the temperature difference between the warm surface seawater and the cold deep seawater in order to produce electricity by the mean of a close or an open thermodynamic cycle. Above the different conversion processes that have been studied, the Organic Rankine Cycle (ORC) appears to be one of the simplest, the most reliable and with relatively low investment and maintenance cost [3].

This resource is available in the tropical belt, where the temperature difference between surface and deep seawater is sufficient (ideally greater than 20 °C) and where this temperature difference is reached close enough from the coastline (depending on the bathymetric profile). Tropical islands are particularly well adapted to OTEC applications. For example, in Reunion Island, the surface seawater temperature shows yearly variations between 23 °C in winter and 28 °C in summer, as observed in the ten-year measurement campaign conducted by the ECOMAR Laboratory [4] (*cf.* Fig. 1). These variations are very repeatable and predictable. Moreover, at a one-day time scale, Fig. 2 shows that the hot seawater temperature can be considered as a constant. On the other hand, the cold deep seawater presents a constant temperature during all the year. For all of these reasons, OTEC is considered to be a base mean of production of electricity that can replace a standard thermal power plant, for example.

Beyond the steadiness of the resource, the study of the dynamic behaviour of an OTEC system is of major interest for various reasons. Firstly, the use of a dynamic model can help to design the strategies for start-up or shut-down operations. Secondly, in Reunion Island, intermittent renewable energies, such as solar, show a very high penetration rate on the electric network, as shown in Fig. 3. These intermittences can disrupt the stability of the electric network, because the production is not well correlated to the consumption. For this reason, the French government is limiting the use of intermittent resources [5], [6]. This assumption shows that having a good knowledge about the controllability of the means of production is an essential need for the manager of an electrical network, in particular for island environments. Contrary to a standard thermal power

plant for which the response time is relatively long, OTEC is using a quasi-infinite hot source at a constant temperature, and the response time of a such system is possibly short enough to allow regulating the network when necessary. The dynamic behaviour of an ORC applied to OTEC has been analysed by Kayton [7] to study the dynamic power response caused by ship heave, in the case of a floating OTEC and to determine better driving strategies. A dynamic model for an OTEC system was also developed by Bai *et al.* [8], but they were considering the Uehara thermodynamic cycle instead of an ORC. They obtained relatively short response times after a step change in mass flow rate (about 200 s).

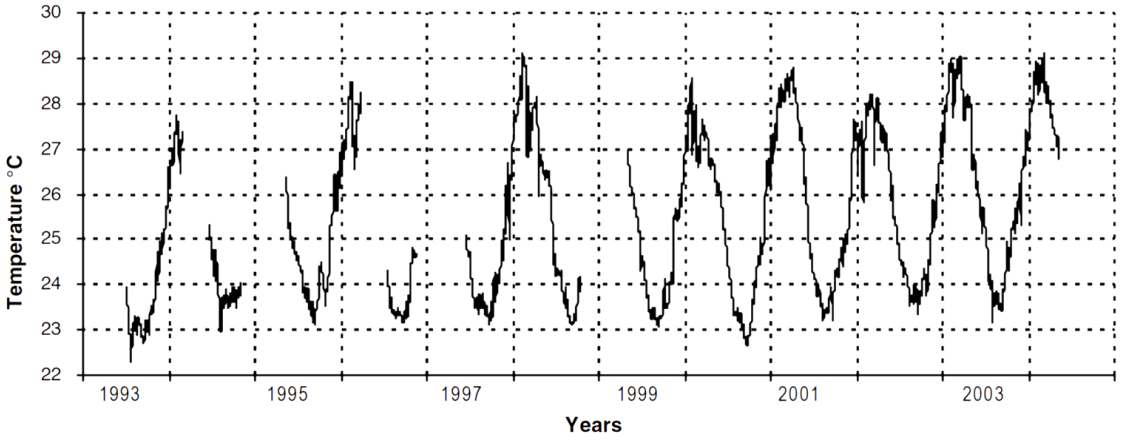

Fig. 1. Evolution of surface seawater temperatures over a 10-year period (source: [4])

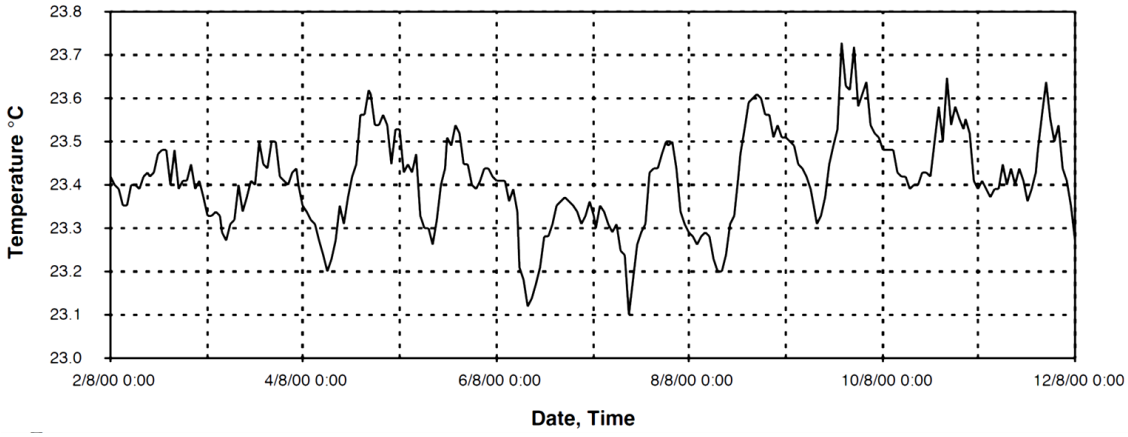

Fig. 2. Evolution of surface seawater temperatures over a 10-day period (source: [4])

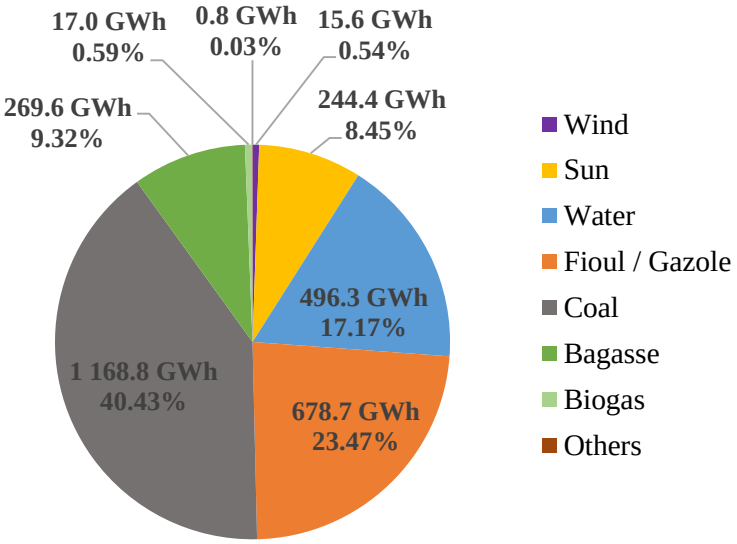

Fig. 3. Total electricity production (Source: ALBIOMA BR / ALBIOMA GOL / EDF - Author: oer [9])

Some research has already been held about the dynamic modelling of ORC systems. The most common approach consists in using separate models for each component of the installation: the heat exchangers (evaporator and condenser), the pump and the turbine [10]. The dynamics of the pump and the turbine are often neglected compared to that of heat exchangers, therefore steady-state models can be used for this two components [11]. Hence, heat exchangers are the key components that determine the transient behaviour of the system. D. Wei *et al.* [10] studied the transient behaviour of an ORC applied to Waste Heat Recovery by comparing two alternative approaches for the representation of heat exchangers: the Moving Boundary Model (MBM) and the discretization technique. They obtained that the two approaches show similar results but with lower calculation time for the MBM approach. This method was also used by other authors [12]–[15] and shows good numerical robustness and efficiency. However, in this three studies, the research focussed on the working fluid side behaviour, and the temperature in the heat fluid side was considered as uniform.

In this study, a dynamic model of an OTEC system is proposed based on steady state models for the pump and the turbine and on the MBM for heat exchangers. Working fluid, exchange surface and heat fluid temperatures variations are considered in each zone. The characteristics of a 10 kW OTEC onshore prototype, located in Reunion Island, are used as parameters for simulations. A first estimation of the response time following a working fluid step change in mass flow rate will then be given.

2 MODEL DESCRIPTION

2.1 Cycle description

The ORC is mainly composed of four components: an evaporator, a condenser, a pump and a turbine. This components are connected by pipes. A throttling valve can also be added before the turbine in order to regulate the vapour mass flow rate. The working fluid at liquid state enters the evaporator (E) where it receives heat from the hot surface seawater and evaporates. The pressurised vapour is then expanded threw the turbine (T), delivering useful work. In the condenser (C), the vapour condenses by releasing heat to the cold seawater. Finally, the pump (P) brings back the liquid to the evaporator.

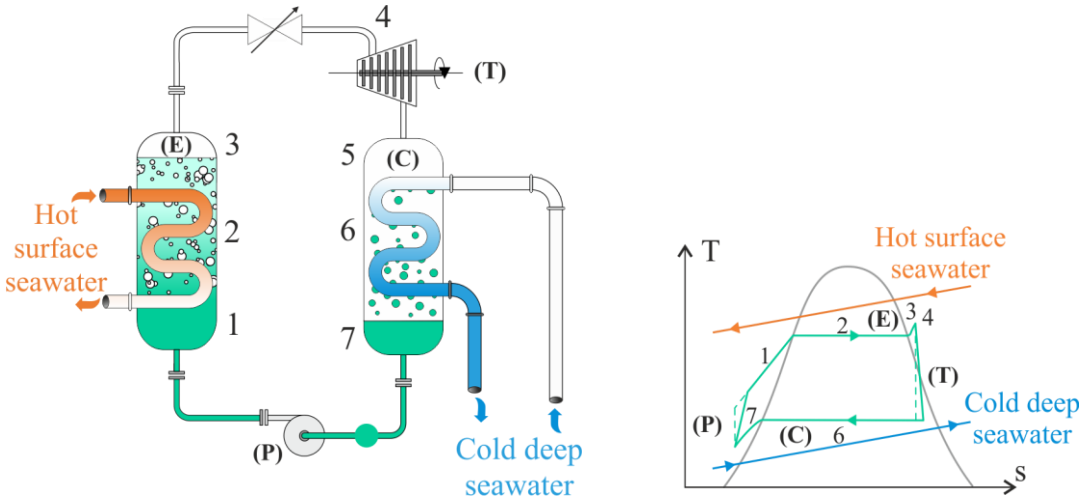

Fig. 4. Schematic representation of an ORC and T-s diagram.

2.2 Evaporator

In the evaporator, the transformation is decomposed into three parts:

- the heating: the subcooled liquid is heated up to the saturation curve (1),
- the evaporation: the phase change process (2),
- the overheating: the vapour is heated (3).

These three parts of the process have to be discriminated, mainly because of the heat transfer coefficients that are significantly different in each part. However, the size of these parts can vary with time, as they depends on the mass flows rates and the amount of heat exchanged. The MBM consists

in integrating the equations of mass and energy conservation in the three parts of the heat exchanger by considering the time dependence of the boundary position.

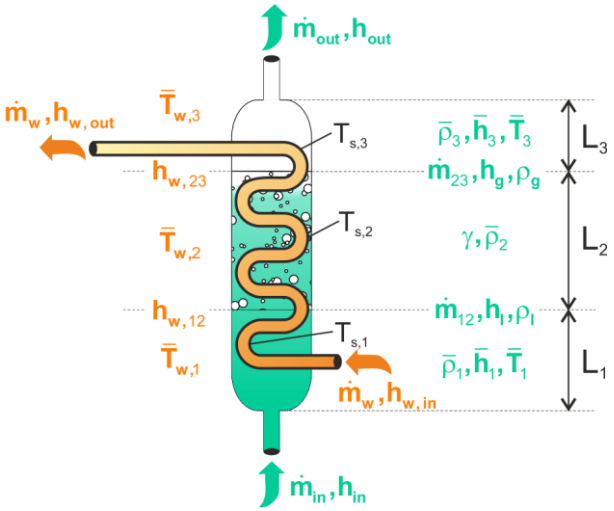

Fig. 5. Schematic of the general MBM and nomenclature of the variables of the evaporator.

2.2.1 Working fluid mass conservation

The local mass conservation equation can be written as:

$$\frac{\partial(A\rho)}{\partial t}+\frac{\partial \dot{m}}{\partial z}=0 \tag{1}$$

The integration of this equation in the heating zone gives:

$$\int_0^{L_1(t)}\frac{\partial(A\rho)}{\partial t}dz+\int_0^{L_1(t)}\frac{\partial \dot{m}}{\partial z}dz=0 \tag{2}$$

By using the Leibniz's rules for differentiation of integrals with time dependant bounds:

$$A\frac{\partial}{\partial t}\int_0^{L_1(t)}\rho dz-A\rho_l\frac{dL_1}{dt}+\dot{m}_{12}-\dot{m}_{in}=0 \tag{3}$$

The mean value of the state variables (volumic mass and enthalpy) are defined by:

$$\overline{h_1}=\frac{h_{in}+h_l}{2} \tag{4}$$

$$\overline{\rho_1}=\frac{1}{L_1}\int_0^{L_1}\rho dz\approx\rho(P,\overline{h_1}) \tag{5}$$

By injecting equations (4) and (5) into equation (3):

$$A(\overline{\rho_1}-\rho_l)\frac{dL_1}{dt}+AL_1\frac{d\overline{\rho_1}}{dt}+\dot{m}_{12}-\dot{m}_{in}=0 \tag{6}$$

All the derivatives can be expressed as a function of two independent state variables. For this study, the chosen variables are specific enthalpy h and pressure P:

$$\begin{aligned}\frac{d\overline{\rho_1}}{dt}&=\left.\frac{\partial\overline{\rho_1}}{\partial P}\right|_{\overline{h_1}}\frac{dP}{dt}+\left.\frac{\partial\overline{\rho_1}}{\partial\overline{h_1}}\right|_P\frac{d\overline{h_1}}{dt}=\left.\frac{\partial\overline{\rho_1}}{\partial P}\right|_{\overline{h_1}}\frac{dP}{dt}+\frac{1}{2}\left.\frac{\partial\overline{\rho_1}}{\partial\overline{h_1}}\right|_P\frac{dh_{in}}{dt}+\frac{1}{2}\left.\frac{\partial\overline{\rho_1}}{\partial\overline{h_1}}\right|_P\frac{dh_l}{dt}\\&=\left(\left.\frac{\partial\overline{\rho_1}}{\partial P}\right|_{\overline{h_1}}+\frac{1}{2}\left.\frac{\partial\overline{\rho_1}}{\partial\overline{h_1}}\right|_P\frac{dh_l}{dP}\right)\frac{dP}{dt}+\frac{1}{2}\left.\frac{\partial\overline{\rho_1}}{\partial\overline{h_1}}\right|_P\frac{dh_{in}}{dt}\end{aligned} \tag{7}$$

Finally, the mass conservation equation in the heating zone can thus be written as:

$$A(\overline{\rho_1}-\rho_l)\frac{dL_1}{dt}+AL_1\left(\left.\frac{\partial\overline{\rho_1}}{\partial P}\right|_{\overline{h_1}}+\frac{1}{2}\left.\frac{\partial\overline{\rho_1}}{\partial\overline{h_1}}\right|_P\frac{dh_l}{dP}\right)\frac{dP}{dt}+\frac{1}{2}AL_1\left.\frac{\partial\overline{\rho_1}}{\partial\overline{h_1}}\right|_P\frac{dh_{in}}{dt}=\dot{m}_{in}-\dot{m}_{12} \tag{8}$$

By a similar development, the mass conservation in the evaporation zone is given by:

$$AL_2\left(\bar{\gamma}\frac{\mathrm{d}\rho_g}{\mathrm{dP}} + (1-\bar{\gamma})\frac{\mathrm{d}\rho_l}{\mathrm{dP}}\right)\frac{\mathrm{dP}}{\mathrm{dt}} + A\left(\rho_l - \rho_g\right)\frac{dL_1}{dt} + A(1-\bar{\gamma})\left(\rho_l - \rho_g\right)\frac{dL_2}{dt} = \dot{m}_{12} - \dot{m}_{23} \quad (9)$$

With $\bar{\gamma}$ the mean vapour quality in the evaporation zone. This parameter is assumed to be constant, assuming that the vapour quality profile among the heat exchanger does not depend on time. We thus have:

$$\overline{\rho_2} = \bar{\gamma}\rho_g + (1-\bar{\gamma})\rho_l \quad (10)$$

In the overheating zone, the mass conservation is given by:

$$AL_3\left(\frac{\partial\overline{\rho_3}}{\partial \mathrm{P}}\Big|_{\overline{h_3}} + \frac{1}{2}\frac{\partial\overline{\rho_3}}{\partial\overline{h_3}}\Big|_P\frac{\mathrm{dh_g}}{\mathrm{dP}}\right)\frac{dP}{dt} + \frac{1}{2}AL_3\frac{\partial\overline{\rho_3}}{\partial\overline{h_3}}\Big|_P\frac{\mathrm{dh_{out}}}{\mathrm{dt}} + A\left(\rho_g - \rho_3\right)\frac{dL_1}{dt} + A\left(\rho_g - \rho_3\right)\frac{dL_2}{dt} = \dot{m}_{23} - \dot{m}_{out} \quad (11)$$

With:

$$\overline{h_3} = \frac{h_g + h_{out}}{2} \quad (12)$$

$$\overline{\rho_3} = \frac{1}{L_3}\int_{L_1+L_2}^{L_3}\rho dz \approx \rho(P, \overline{h_3}) \quad (13)$$

2.2.2 Working fluid energy conservation

The local energy conservation equation can be written as:

$$\frac{\partial(A\rho h - AP)}{\partial t} + \frac{\partial\dot{m}h}{\partial z} = q \quad (14)$$

Where $q = dQ/dz$ is the linear amount of heat exchanged expressed in W.m^{-1}.

The integration in each zone gives:

- Heating zone:

$$AL_1\left\{\overline{h_1}\left(\frac{\partial\overline{\rho_1}}{\partial \mathrm{P}}\Big|_{\overline{h_1}} + \frac{1}{2}\frac{\partial\overline{\rho_1}}{\partial\overline{h_1}}\Big|_{\mathrm{P}}\frac{\mathrm{dh_l}}{\mathrm{dP}}\right) + \frac{1}{2}\overline{\rho_1}\frac{\mathrm{dh_l}}{\mathrm{dP}} - 1\right\}\frac{\mathrm{dP}}{\mathrm{dt}} + \left(\frac{1}{2}AL_1\overline{h_1}\frac{\partial\overline{\rho_1}}{\partial\overline{h_1}}\Big|_{\mathrm{P}} + \frac{1}{2}AL_1\overline{\rho_1}\right)\frac{\mathrm{dh_{in}}}{\mathrm{dt}} + A\left(\overline{\rho_1}\overline{h_1} - \rho_l h_l\right)\frac{dL_1}{dt} = Q_1 + \dot{m}_{in}h_{in} - \dot{m}_{12}h_l \quad (15)$$

- Evaporation zone:

$$AL_2\left((1-\bar{\gamma})\frac{\mathrm{d\rho_l}h_l}{\mathrm{dP}} + \bar{\gamma}\frac{\mathrm{d\rho_g}h_g}{\mathrm{dP}} - 1\right)\frac{\mathrm{dP}}{\mathrm{dt}} + A\left(\rho_l h_l - \rho_g h_g\right)\frac{dL_1}{dt} + A(1-\bar{\gamma})\left(\rho_l h_l - \rho_g h_g\right)\frac{dL_2}{dt} = Q_2 + \dot{m}_{12}h_l - \dot{m}_{23}h_g \quad (16)$$

- Overheating zone:

$$AL_3\left\{\overline{h_3}\left(\frac{\partial\overline{\rho_3}}{\partial P}\Big|_{\overline{h_3}} + \frac{1}{2}\frac{\partial\overline{\rho_3}}{\partial\overline{h_3}}\Big|_P\frac{dh_g}{dP}\right) + \frac{1}{2}\overline{\rho_3}\frac{dh_g}{dP} - 1\right\}\frac{dP}{dt} + \frac{1}{2}AL_3\left(\overline{h_3}\frac{\partial\overline{\rho_3}}{\partial\overline{h_3}}\Big|_P + \overline{\rho_3}\right)\frac{dh_{out}}{dt} + A\left(\rho_g h_g - \overline{\rho_3}\overline{h_3}\right)\frac{dL_1}{dt} + A\left(\rho_g h_g - \overline{\rho_3}\overline{h_3}\right)\frac{dL_2}{dt} = Q_3 + \dot{m}_{23}h_g - \dot{m}_{out}h_{out} \quad (17)$$

Where the amount of heat transferred from the surface to the working fluid in the zone $i \in \{1; 2; 3\}$ is given by:

$$Q_i = \alpha_i S_i (T_{si} - \overline{T_i}) \tag{18}$$

Where α_i is the heat transfer coefficient and S_i the heat exchange surface, depending on the size of the zone L_i.

2.2.3 Energy conservation for the exchange surface

Because the heat exchange surface is solid, the energy conservation threw this surface can be written:

$$c_s \rho_s A_s \frac{\partial T_s}{\partial t} = q_w - q \tag{19}$$

The integration gives:

- In the heating zone:

$$c_s \rho_s A_s \left(\overline{T_{s1}} - T_s(L_1)\right) \frac{dL_1}{dt} + c_s \rho_s A_s L_1 \frac{d\overline{T_{s1}}}{dt} = Q_{w1} - Q_1 \tag{20}$$

- In the evaporation zone:

$$\begin{aligned} c_s \rho_s A_s \left(\overline{T_{s2}} - T_s(L_1 + L_2)\right) \frac{dL_2}{dt} + c_s \rho_s A_s \left(T_s(L_1) - T_s(L_1 + L_2)\right) \frac{dL_1}{dt} + c_s \rho_s A_s L_2 \frac{d\overline{T_{s2}}}{dt} \\ = Q_{w2} - Q_2 \end{aligned} \tag{21}$$

- In the overheating zone:

$$\begin{aligned} c_s \rho_s A_s (T_s(L_1 + L_2) - \overline{T_{s3}}) \frac{dL_1}{dt} + c_s \rho_s A_s (T_s(L_1 + L_2) - \overline{T_{s3}}) \frac{dL_2}{dt} + c_s \rho_s A_s L_3 \frac{d\overline{T_{s3}}}{dt} \\ = Q_{w3} - Q_3 \end{aligned} \tag{22}$$

2.2.4 Water side mass and energy conservation

The water is considered as an incompressible fluid, hence, the mass conservation is traduced by the conservation of the mass flow rate among the pipes and heat exchangers. Moreover, pressure losses are neglected. Thus, only the energy conservation equations in each zone are considered:

- In the heating zone:

$$\begin{aligned} \frac{1}{2} A \rho_w L_1 \frac{dh_{w,in}}{dt} + \frac{1}{2} A \rho_w L_1 \frac{dh_{w,12}}{dt} + A\left(\rho_w \overline{h_{w,1}} - \rho_w h_{w,12}\right) \frac{dL_1}{dt} - A L_1 \frac{dP_w}{dt} \\ = Q_{w1} + \dot{m}_w \left(h_{w,in} - h_{w,12}\right) \end{aligned} \tag{23}$$

- In the evaporation zone:

$$\begin{aligned} \frac{1}{2} A \rho_w L_2 \frac{dh_{w,12}}{dt} + \frac{1}{2} A \rho_w L_2 \frac{dh_{w,23}}{dt} + A\left(\rho_w h_{w,12} - \rho_w h_{w,23}\right) \frac{dL_1}{dt} \\ + A\left(\rho_w \overline{h_{w,2}} - \rho_w h_{w,23} + P_{w,23} - \overline{P_{w,2}}\right) \frac{dL_1}{dt} - A L_2 \frac{dP_w}{dt} \\ = Q_{w2} + \dot{m}_w \left(h_{w,12} - h_{w,23}\right) \end{aligned} \tag{24}$$

- In the overheating zone:

$$\begin{aligned} \frac{1}{2} A \rho L_3 \frac{dh_{w,out}}{dt} + \frac{1}{2} A \rho L_3 \frac{dh_{w,23}}{dt} + A\left(\rho_w h_{w,23} - \rho_w \overline{h_{w,3}}\right) \frac{dL_1}{dt} \\ + A\left(\rho_w h_{w,23} - \rho_w \overline{h_{w,3}} + \overline{P_{w,2}} - P_{w,23}\right) \frac{dL_2}{dt} - A L_3 \frac{dP_w}{dt} \\ = Q_{w3} + \dot{m}_w \left(h_{w,23} - h_{w,out}\right) \end{aligned} \tag{25}$$

Equations (8), (9), (11), (15), (16), (17), (20), (21), (22), (23), (24) and (25) constitute a system of 12 coupled differential equations, with 12 state variables: P, L_1, L_2, $\dot{m}_{12}$, $\dot{m}_{23}$, h_{out}, $\overline{T_{s1}}$, $\overline{T_{s2}}$, $\overline{T_{s3}}$, $h_{w,12}$, $h_{w,23}$, $h_{w,out}$. Input parameters are $\dot{m}_{in}$, h_{in}, $\dot{m}_w$, $h_{w,in}$ and P_w, which are given by the working fluid pump and water conditions.

2.3 Condenser

The model for the condenser is similar to that of the evaporator, excepted that the three zones are desuperheating (5), condensation (6) and subcooling (7). As the first zone may not exist during nominal operation, the system is written in two forms: one with three zone and one with just the two last zones. A test on the state of the fluid at the condenser inlet may define which system will be solved by the program.

2.4 Pump

As the response time for the pump is much faster than that of heat exchangers, a static model is used to describe this component. The liquid mass flow rate is given by:

$$\dot{m}_{pump} = \eta_v V_{cyl} \rho_{in} \omega \tag{26}$$

Where η_v is the volumetric efficiency, V_{cyl} is the cylinder volume, ρ_{in} the volumic mass of the fluid at the inlet of the pump and ω is the rotational speed.

The enthalpy change during the transformation is given by the isentropic efficiency of the pump:

$$\eta_{pump} = \frac{\Delta h_{pump}^{is}}{\Delta h_{pump}} \tag{27}$$

Where Δh_{pump}^{is} is the enthalpy change in the pump in the case of an isentropic process and Δh_{pump} is the real enthalpy change in the pump.

2.5 Turbine

In the same way as the pump, a static model is used for the turbine. The vapour mass flow rate is given by (see [16]):

$$\dot{m}_{turb} = C_v \sqrt{\rho_3 \left(P_{in,turb} - P_{cond} \right)} \tag{28}$$

The inlet pressure of the turbine can be the evaporator pressure or lower depending on the opening of the throttling valve. The objective of this throttling valve is to ensure that the vapour mass flow rate is the same as the liquid mass flow rate.

The enthalpy change is determined by:

$$\eta_{turb} = \frac{\Delta h_{turb}}{\Delta h_{turb}^{is}} \tag{29}$$

3 CASE STUDY: SIMULATION OF A STEP CHANGE IN MASS FLOW RATE

The model described in the previous part is used in order to determine a first order of magnitude of the response time of an OTEC plant. As input parameters, data from the onshore OTEC prototype located in Reunion Island have been used. The evaporator is a flooded shell-and-tube one and the condenser is a smooth shell-and-tube one. The working fluid is ammonia (R717). This prototype is presented in details by Castaing *et al.* [17]. Heat transfer coefficients are taken equal to orders of magnitude of those obtained on this prototype.

3.1 Simulation hypothesis

Heat losses and pressure drops are neglected. The characteristics of the different components are listed in Table 1. The simulation consists in considering the system initially in steady state which will undergo a modification of the flow of the working fluid after a time t = 300 s. The initial operating values are given in Table 2. At t = 300 s, the rotational speed of the pump is reduced by 25 %. The working fluid mass flow rate then undergoes a decreasing step change from 0.339 kg/s to 0.255 kg/s. The throttling valve is assumed to regulate the pressure at the inlet of the turbine so as to maintain the gas mass flow rate equal to the liquid mass flow rate at each time.

Table 1. Input parameters used for the simulation

Parameter	Value	Parameter	Value
Evaporator (Water side)		*Condenser (Water side)*	
Heat Transfer Coefficient h_w	6000 W.m^{-2}.K^{-1}	Heat Transfer Coefficient h_w	6000 W.m^{-2}.K^{-1}
Evaporator (Working Fluid side)		*Condenser (Working Fluid side)*	
Heat Transfer Coefficient h_1	500 W.m^{-2}.K^{-1}	Heat Transfer Coefficient h_1	1000 W.m^{-2}.K^{-1}
Heat Transfer Coefficient h_2	8000 W.m^{-2}.K^{-1}	Heat Transfer Coefficient h_2	9000 W.m^{-2}.K^{-1}
Heat Transfer Coefficient h_3	1000 W.m^{-2}.K^{-1}	Heat Transfer Coefficient h_3	500 W.m^{-2}.K^{-1}
Evaporator (Heat Exchange Surface)		*Condenser (Heat Exchange Surface)*	
Volumic mass ρ_s	8960 kg.m^{-3}	Volumic mass ρ_s	8960 kg.m^{-3}
Heat Capacity C_s	385 J.K^{-1}.kg^{-1}	Heat Capacity C_s	385 J.K^{-1}.kg^{-1}
Pump		*Turbine*	
Volumetric efficiency η_v	0.6	Flow coefficient C_V	2.12×10^{-4} m^2
Cylinder volume V_{cyl}	1.80×10^{-5} m^3	Isentropic efficiency η_{turb}	0.8
Isentropic efficiency η_{pump}	0.8		

Table 2. Initial steady state operating values

Parameter	Value	Parameter	Value
Evaporator (Water side)		*Condenser (Water side)*	
Water mass flow rate $\dot{m}_w$	40 kg/s	Water mass flow rate $\dot{m}_w$	30 kg/s
Inlet water temperature $T_{w,in}$	28 °C	Inlet water temperature $T_{w,in}$	5 °C
Outlet water temperature $T_{w,out}$	26.09 °C	Outlet water temperature $T_{w,out}$	7.43 °C
Evaporator (Working Fluid side)		*Condenser (Working Fluid side)*	
Working fluid mass flow Rate $\dot{m}_w$	0.339 kg/s	Working fluid mass flow Rate $\dot{m}_w$	0.339 kg/s
Inlet liquid temperature T_{in}	8.36 °C	Inlet liquid temperature T_{in}	9.28 °C
Outlet vapour temperature T_{out}	26.55 °C	Outlet vapour temperature T_{out}	8.25 °C
Pressure P	9.5 bar	Pressure P	6 bar
Pump			
Rotational speed ω	50 Hz		

3.2 Results and discussion

Fig. 6 shows the evolution of the different variables during the dynamic simulation. The response time following the step change in mass flow rate in terms of pressure and temperature is relatively short. The temperature variation is lower than 0.1 °C/min after 2 minutes. Pressure in the evaporator increases while pressure in the condenser decreases, therefore the energy efficiency increases but the pinch point in heat exchangers decreases. The size of the different zones do not undergo great variations, but the evaporating zone is smoothly increasing. The power output varies from 15.7 kW to 13.7 kW. A decreasing step change in working fluid mass flow rate of 25 % thus causes a decreases in terms of power output of 12.7 %.

This results show that the power output of an OTEC power plant can be easily adjusted with short response times by piloting the working fluid pump rotational speed and the throttling valve upstream the turbine, without changing the operation of the seawater pumps. However, the response in terms of relative power variation are near to half than the relative mass flow rate variation (12.7 % against 25 %). The modulation of the power by this method is thus limited, because the frequency of the pump has to be kept in its operation range. If the power has to be modified with a larger amplitude, a modification of the seawater mass flow rate will be necessary.

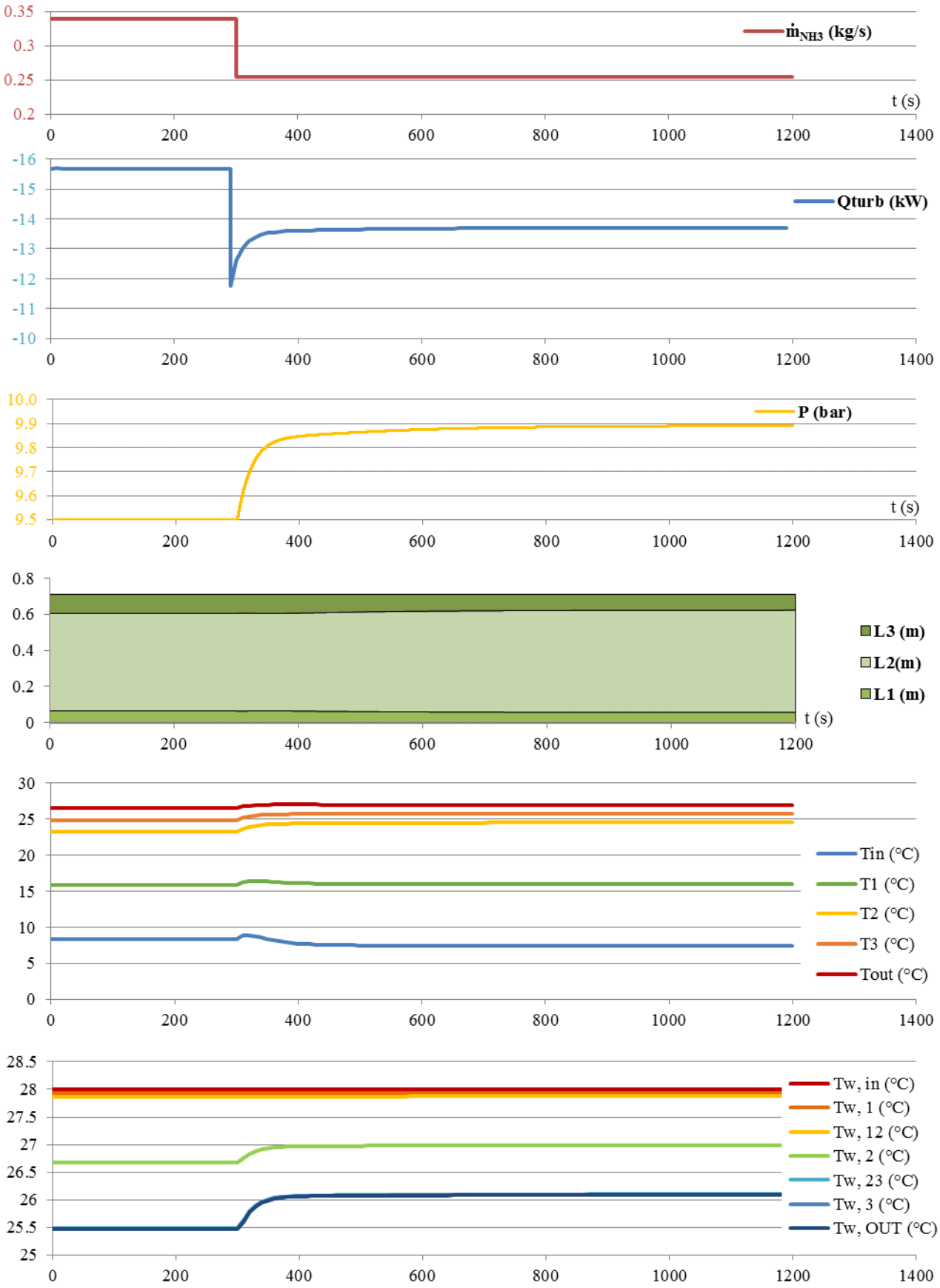

Fig. 6. Evolution of the different state variables of the evaporator during the simulation

4 CONCLUSION AND PERSPECTIVES

In this study, a dynamic model of an ORC applied to OTEC is presented. Heat exchangers are described by the MBM (Moving Boundary Model) and by considering variations of both heat and working fluid temperature in each zone. Simulations were conducted by using input parameters from an OTEC Onshore Prototype located in Reunion Island. The response of the system following a step change in working fluid mass flow rate is studied, and shows that the power output of an OTEC power plant can be adjusted with relatively short response times (lower than two minutes in this case from 15.7 kW to 13.7 kW).

These results are encouraging in the idea that an OTEC system could be used not only as a stable base energy resource, but also as an innovative way to regulate the electric network in sensible zones (such as non-connected islands). However, control-command strategies have to be designed by considering both working fluid and seawater mass flow rates in order to give the possibilities of such a system. Response times for larger scale systems have also to be studied.

ACKNOWLEDGMENTS

The authors would like to thank Réunion Region and NAVAL Energies for funding this research.

NOMENCLATURE

A	section, m^2
c	specific heat capacity, J/(kg.K)
h	specific enthalpy, J/kg
L	length, m
$\dot{m}$	mass flow rate, kg/s
P	pressure, Pa
q	linear heat power, W/m
Q	heat power, W
t	time, s
T	temperature, K
V	volume, m^3

Greek symbols

α	heat transfer coefficient, $W/(m^2 K)$
γ	vapour quality
η	efficiency
ρ	density, kg/m^3
ω	rotational speed, rad/s

Subscripts and superscripts

in	inlet
out	outlet
l	saturated liquid
g	saturated gas
1	zone 1
2	zone 2
3	zone 3
12	interface between zone 1 and 2
23	interface between zone 2 and 3
s	heat exchange surface of the heat exchanger
w	water
v	volumetric
cyl	cylinder
is	isentropic
turb	turbine
cond	condenser

REFERENCES

[1] M. S. Quinby-Hunt, D. Sloan, et P. Wilde, « Potential environmental impacts of closed-cycle ocean thermal energy conversion », *Environmental Impact Assessment Review*, vol. 7, nº 2, p. 169–198, 1987.

[2] W. H. Avery et C. Wu, « Renewable energy from the ocean-A guide to OTEC », 1994.

[3] J. Bao et L. Zhao, « A review of working fluid and expander selections for organic Rankine cycle », *Renewable and Sustainable Energy Reviews*, vol. 24, p. 325‑342, août 2013.

[4] F. Conand, F. Marsac, E. Tessier, et C. Conand, « A ten-year period of daily sea surface temperature at a coastal station in Reunion Island, Indian Ocean (July 1993–April 2004): patterns of variability and biological responses », *Western Indian Ocean Journal of Marine Science*, vol. 6, nº 1, 2008.

[5] J. P. Praene, M. David, F. Sinama, D. Morau, et O. Marc, « Renewable energy: Progressing towards a net zero energy island, the case of Reunion Island », *Renewable and Sustainable Energy Reviews*, vol. 16, nº 1, p. 426‑442, janv. 2012.

[6] M. Drouineau, E. Assoumou, V. Mazauric, et N. Maïzi, « Increasing shares of intermittent sources in Reunion Island: Impacts on the future reliability of power supply », *Renewable and Sustainable Energy Reviews*, vol. 46, nº Supplement C, p. 120‑128, juin 2015.

[7] M. Kayton, « Steady-State and Dynamic Performance of an Otec Plant », *IEEE Transactions on Power Apparatus and Systems*, vol. PAS-100, nº 3, p. 1148‑1153, mars 1981.

[8] O. Bai, M. Nakamura, Y. Ikegami, et H. Uehara, *Simulation and Evaluation of Transient Performance of Ocean Thermal Energy Conversion Plant with Working Fluid of Binary Mixtures*. 2017.

[9] Energies Réunion SPL, « Bilan Energétique - Île de La Réunion 2015 ». OER, 2016.

[10] D. Wei, X. Lu, Z. Lu, et J. Gu, « Dynamic modeling and simulation of an Organic Rankine Cycle (ORC) system for waste heat recovery », *Applied Thermal Engineering*, vol. 28, nº 10, p. 1216‑1224, juill. 2008.

[11] S. Quoilin, R. Aumann, A. Grill, A. Schuster, V. Lemort, et H. Spliethoff, « Dynamic modeling and optimal control strategy of waste heat recovery Organic Rankine Cycles », *Applied energy*, vol. 88, nº 6, p. 2183–2190, 2011.

[12] J. Zhang, W. Zhang, G. Hou, et F. Fang, « Dynamic modeling and multivariable control of organic Rankine cycles in waste heat utilizing processes », *Computers & Mathematics with Applications*, vol. 64, nº 5, p. 908–921, 2012.

[13] W.-J. Zhang et C.-L. Zhang, « A generalized moving-boundary model for transient simulation of dry-expansion evaporators under larger disturbances », *International Journal of Refrigeration*, vol. 29, nº 7, p. 1119–1127, 2006.

[14] M. Willatzen, N. Pettit, et L. Ploug-Sørensen, « A general dynamic simulation model for evaporators and condensers in refrigeration. Part I: moving-boundary formulation of two-phase flows with heat exchange: Modèle général dynamique pour évaporateurs et condenseurs frigorifiques. Partic I: Formulation des conditions aux limites variables de flux biphasiques avec échange de chaleur », *International Journal of refrigeration*, vol. 21, nº 5, p. 398–403, 1998.

[15] T. L. McKinley et A. G. Alleyne, « An advanced nonlinear switched heat exchanger model for vapor compression cycles using the moving-boundary method », *International Journal of refrigeration*, vol. 31, nº 7, p. 1253–1264, 2008.

[16] J. M. Jensen et H. Tummescheit, « Moving boundary models for dynamic simulations of two-phase flows », in *Proceedings of the 2nd International Modelica Conference*, 2002, p. 235–244.

[17] F. Sinama *et al.*, « Etude expérimentale d'un prototype ETM à La Réunion », in *Congrès Français de Thermique 2016*, 2016.